

# Evaluation of Synthesis Variables on the Antimicrobial and Antioxidant Efficacy of Silver Nanoparticles Produced Using *Hibiscus sabdariffa* Extract

Hasan Basari<sup>1</sup>, Mustafa Yontem<sup>1,2\*</sup> , Fatih Erci<sup>1,\*</sup> , Busra Esirgenler<sup>1</sup> 

<sup>1</sup> Department of Biotechnology, Faculty of Science, Necmettin Erbakan University, Meram-Konya, Turkey; hasanb0096@gmail.com (H.B.); ferci@erbakan.edu.tr (F.E.); busraesirgenler@gmail.com (B.E.);

<sup>2</sup> Department of Nursing, Faculty of Health Science, Karamanoğlu Mehmetbey University, Karaman, Turkey; mustafayontem@kmu.edu.tr (M.Y.);

\* Correspondence: mustafayontem@kmu.edu.tr (M.Y.); ferci@erbakan.edu.tr (F.E.);

Scopus Author ID 56708760300

Received: 14.01.2024; Accepted: 7.07.2024; Published: 14.02.2025

**Abstract:** The increasing interest in biological synthesis techniques can be attributed to the need for non-toxic ways to produce nanoparticles. This study investigated the influence of different parameters on the synthesis of silver nanoparticles (AgNPs) using *Hibiscus sabdariffa* extract. Several analytical techniques were used to characterize the synthesized AgNPs. Furthermore, the antimicrobial and DPPH radical scavenging activities of the AgNPs were evaluated. XRD analysis validated the synthesis of pure nanosized crystalline silver nanoparticles. At room temperature, as the pH rised during the synthesis, the size of the nanoparticles decreased. Additionally, pH had the biggest impact on the distinctive qualities of AgNPs, while extract concentration, metal salt, and pH all affected the nanoparticles' zeta potential. The synthesized AgNPs showed antibacterial activity against Gram-positive and Gram-negative bacteria, with the greatest activity observed against *Staphylococcus aureus*. AgNPs have been shown to have greater antibacterial activity when synthesized at a pH of 7.5, as opposed to pH values of 8.5 and 10.5. To sum up, pH played a significant role in the synthesis of AgNPs and was essential for determining the biological activities of the particles. According to this study, it is possible to control nanoparticle synthesis parameters for applications in various industries, such as the food and medical sectors.

**Keywords:** *Hibiscus sabdariffa*; silver nanoparticles; synthesis parameters; antibacterial activity; antioxidant activity.

© 2025 by the authors. This article is an open-access article distributed under the terms and conditions of the Creative Commons Attribution (CC BY) license (<https://creativecommons.org/licenses/by/4.0/>).

## 1. Introduction

Metal-based nanoparticles (MNPs) have become a significant form of nanomaterials in a variety of biomedical applications due to the rapid advancement of nanotechnology, including drug delivery, bioimaging, and tissue engineering due to their unique properties such as spherical shape, small size, metallic composition, and high surface area [1–4]. Nanoparticles, particularly silver nanoparticles, have demonstrated significant antimicrobial activity against a wide range of microorganisms. Furthermore, silver nanoparticles have been recognized for their effective role in disrupting bacterial membrane permeability [5]. Silver nanoparticles have been proposed to inactivate respiratory chain dehydrogenases in bacteria by disrupting the periplasmic space, permeability, and outer peptidoglycan barrier [6]. It has been demonstrated that smaller-sized nanoparticles have more antibacterial activity against pathogens than larger-

sized nanoparticles [7]. This could be due to smaller nanoparticles' faster transport into cells than larger ones [8].

Additionally, smaller-sized AgNPs provide a larger and more ideal surface area for interaction with various bacterial species [9]. Furthermore, AgNPs can interact with the surface of bacterial membranes and enter bacterial cells [10]. The antimicrobial activity of AgNPs has been shown to be derived from the oxidation of released silver atoms and the release of Ag<sup>+</sup> ions from the surfaces of AgNPs [11].

Non-toxic and environmentally friendly biological methods have garnered significant attention recently compared to physicochemical nanoparticle manufacturing techniques [12–15]. Numerous methods have been developed for the biological or biogenic fabrication of nanoparticles using metal salts. These approaches involve the utilization of microorganisms, plant tissues and fruits, plant extracts, and marine algae as sources for the synthesis of nanoparticles. These biological entities possess inherent capabilities to reduce metal ions and facilitate the formation of nanoparticles [16–20]. Biological synthesis allows for the precise control of size and structure and the production of large quantities of nanoparticles with no environmental impact [21,22]. The use of plant extracts for the synthesis of nanoparticles is considered a more straightforward and cost-effective approach compared to using plant tissues. Plant extracts offer a simpler and more affordable method for nanoparticle synthesis when contrasted with techniques involving microorganisms or whole plants [23]. These advantages have led to increased interest in nanoparticle synthesis using plant extracts [24,25].

Primary and secondary metabolites comprise a broad range of active phytochemicals present in plants. Secondary metabolites have a wide range of biologically relevant characteristics, including potential anticancer activities, antibacterial and antifungal effects, anti-inflammatory properties, and antioxidant activity. These secondary metabolites are essential for plant defense mechanisms and have attracted significant interest for their potential therapeutic uses in various medical and pharmacological sectors [26–28]. The synergy between the activities of secondary metabolites and metal nanoparticles (MNPs) enhances the biocompatibility of phyto-MNPs for various biomedical applications [29]. Secondary metabolites emerge as the principal agents in MNP synthesis, acting as reducing, stabilizing, and coating agents, reducing metal ions to zero-valent MNPs in a single step. In contrast, primary metabolites play an important role in production [2,30]. The strong coating of MNPs ensures their stability against agglomeration and aggregation [31].

The size and shape of nanoparticles can be affected by various chemical and physical factors. Many studies on nanoparticle synthesis have examined various reaction parameters, including temperature, pH, incubation time, aeration, salt content, redox conditions, and agitation speed [32,33]. Variations in the content of plant extracts can affect the amount, size, shape, distribution, and aggregation of phyto-MNPs. A decrease in the plant extract concentration results in the formation of larger-sized nanoparticles, while increasing in concentration leads to smaller, spherical, isotropic, well-dispersed, and agglomeration-free phyto-MNPs [34,35]. The distribution and size of phyto-MNPs can be affected by external elements such as light, pH, and oxygen, which can also affect the effectiveness of the active ingredients. The zeta potential, size, and intensity of the SPR peak of phyto-MNPs are all affected by pH, which also has an impact on the reducing ability of phyto-components, the release of protons from the surface of NPs, and other variables [36].

This research aimed to produce silver nanoparticles utilizing the extract obtained from the plant *Hibiscus sabdariffa*. The synthesized nanoparticles were subjected to a

comprehensive characterization process involving several spectroscopic and microscopic techniques. The study focused on examining the influence of various synthesis parameters on the distinctive properties of the nanoparticles, as well as their antimicrobial and antioxidant activities.

## 2. Materials and Methods

### 2.1. Preparation of the plant extract.

The plant sample (*Hibiscus sabdariffa* L.) used for the synthesis of silver nanoparticles was supplied by Doğan Baharatçılık. The plant sample was first ground in a grinder for approximately 10 min. Then, 5 g of the ground plant material was weighed and mixed with 100 mL of distilled water. To obtain the aqueous extract of the plant, the mixture was placed in a water bath at 80°C and gently stirred at 5-minute intervals for 2 h. Then, the mixture was filtered using a paper filter to separate it from the residue. The filtration process was repeated twice to remove large particles from the extract completely. The prepared extract was stored in bottles, with no contact with air, at +4°C in refrigerators.

### 2.2. Synthesis of silver nanoparticles.

The synthesis of silver nanoparticles (AgNPs) involved the investigation of various parameters, including pH, temperature, AgNO<sub>3</sub> concentration, extract concentration, and incubation time. To synthesize AgNPs, the aqueous solution of AgNO<sub>3</sub> (300 mL) was mixed with *Hibiscus sabdariffa* L. plant extract in a suitable bottle. The mixture was agitated at 1200 rpm using a shaker, and UV-Vis spectrophotometry measurements were taken at regular intervals. The reduction of silver ions resulted in a color change from red to dark brown in the solution. Subsequently, the dark-colored solution was centrifuged at 9000 rpm at 4°C for 15 min. to separate the upper liquid phase. Then, centrifugation was repeated three times to wash the solution using distilled water. The obtained solid portion was stored at +4°C for further characterization of the AgNPs.

### 2.3. Characterization of silver nanoparticles.

The characterization of AgNPs involved the use of various analytical instruments. The UV-Vis spectra of AgNPs were recorded using a Cary 60 UV-Vis spectrophotometer (Agilent Technologies, Santa Clara, CA, USA) in the 200 to 800 nm wavelength range. The obtained data were analyzed and plotted using Origin 8.5 software (OriginLab, Northampton, MA, USA). Fourier transform infrared (FTIR) spectroscopic analysis was conducted using a Shimadzu IR Prestige-21 FTIR-ATR spectrometer to confirm the functional groups involved in synthesizing and stabilizing AgNPs with capping agents. The AgNPs powder was subjected to X-ray diffraction analysis using an X-ray diffraction system (PANalytical Empyrean model, UK) with CuK $\alpha$  radiation ( $k = 1.54$  Å). The XRD pattern was examined with a step size of 0.02, covering the  $2\theta$  range from 10° to 80°. The polydispersity index, hydrodynamic size, and charge of the particles were determined using dynamic light scattering (DLS) and zeta potential measurements performed with a Malvern instrument (Zetasizer nano ZS, Malvern Instruments, UK). To prepare the AgNP suspension for DLS and zeta potential analysis, the particles were obtained by centrifugation, washing, and subsequent sonication for 30 min. at 25°C in ddH<sub>2</sub>O. For TEM analysis, a diluted solution of silver nanoparticles was dropped onto a carbon-coated

copper grid. The samples were then air-dried at room temperature for 24 hours before being examined using a JEOL electron microscope (JEOL 200 FX-II) to observe the nanoparticle morphology. Scanning electron microscopy (SEM) was used for morphological studies, and energy-dispersive X-ray analysis (EDX) with a FESEM instrument (JEOL JSM-7400 F, Tokyo, Japan) was performed to analyze the composition and verify the size and shape of the AgNPs.

#### 2.4. Evaluation of the antimicrobial activity for silver nanoparticles.

Microorganism cultures of *Staphylococcus aureus* (*S. aureus*), *Bacillus cereus* (*B. cereus*), *Salmonella typhimurium* (*S. typhimurium*), *Enterococcus faecalis* (*E. faecalis*), *Pseudomonas aeruginosa* (*P. aeruginosa*), *Escherichia coli* (*E. coli*), *Bacillus subtilis* (*B. subtilis*), and *Aspergillus niger* (*A. niger*) were obtained in lyophilized form. Mueller Hinton Agar (MHA) supplemented with 2% glucose was prepared to determine the antibacterial and antifungal activity. The suspension turbidity of the tested isolates was adjusted to the equivalent of the McFarland 0.5 standard. After homogenization by shaking the liquid cultures, approximately 100  $\mu\text{L}$  volume was poured onto the entire surface of a petri dish and spread using a Drigalski Spatula to ensure even distribution. Wells with a diameter of 7 mm were created in the MHA agar plates, and 50  $\mu\text{L}$  of nanoparticle solution was added to each well. The zone diameters formed around the wells were measured millimeters after 24 h of incubation at 37°C and evaluated. The experiments were performed in triplicate.

#### 2.5. DPPH radical scavenging activity of Hs-AgNPs.

Utilizing 96-well microplates, the DPPH radical scavenging activity was carried out. After making a DPPH radical solution in methanol, 100  $\mu\text{L}$  of this solution was poured into each well. AgNPs and ascorbic acid were added to the wells at a concentration of 400  $\mu\text{g}/\text{mL}$ . The reaction mixture was then thoroughly combined and left to stand at room temperature for 30 minutes in the dark. The absorbance was then measured spectrophotometrically at 517 nm. The decrease in absorption was determined by comparing it with the control. The radical scavenging activity of AgNPs was calculated using the following formula [1].

$$\text{DPPH scavenging efficiency (\%)} = \frac{\text{Abs control} - \text{Abs sample}}{\text{Abs control}} \times 100 \quad [1]$$

### 3. Results and Discussion

#### 3.1. Synthesis of silver nanoparticles.

Silver nanoparticles (AgNPs) were synthesized by combining a silver nitrate solution with plant extract. As the reaction progressed, the color of the solution transitioned from yellow to reddish-brown, indicating the successful formation of AgNPs. This color change is attributed to surface plasmon resonance, where the nanoparticles absorb and scatter light at specific wavelengths. To further characterize the synthesized AgNPs, absorption spectra were obtained using a UV-Vis spectrophotometer at regular 15-minute intervals. The synthesis parameters employed in this investigation, including variations in plant extract concentration, reaction time, and other factors, were deliberately chosen to examine their impact on the formation and properties of the AgNPs. An overview of the synthesis parameters utilized in this study is given in Table 1.

**Table 1.** Synthesis parameters of the silver nanoparticles.

Sample No.	pH	Temperature	AgNO <sub>3</sub> concentration	Plant extract
Hs-AgNPs-1	7.5	25 °C	1 mM	30 mL
Hs-AgNPs-2	8.5	25 °C	1 mM	30 mL
Hs-AgNPs-3	8.5	25 °C	2 mM	30 mL
Hs-AgNPs-4	10.5	25°C	2 mM	30 mL
Hs-AgNPs-5	7.5	50 °C	1 mM	30 mL
Hs-AgNPs-6	8.5	50 °C	1 mM	15 mL
Hs-AgNPs-7	8.5	50 °C	1 mM	30 mL
Hs-AgNPs-8	10.5	50 °C	1 mM	30 mL

The effect of pH, temperature, AgNO<sub>3</sub> concentration, and extract concentration on the synthesis of nanoparticles was investigated. Three different pH values (7.5, 8.5, and 10.5) were utilized to examine their influence on nanoparticle formation. The temperature variation was evaluated by conducting the nanoparticle synthesis at 25°C and 50°C. Different concentrations of AgNO<sub>3</sub> (1 and 2 mM) were employed to investigate the effect of metal ion concentration on nanoparticle synthesis. Two different extract concentrations (15 mL and 30 mL) were selected to assess their impact on nanoparticle synthesis. Eight different synthesis environments were prepared to explore the combined effects of these parameters on nanoparticle synthesis. After the reactions, the samples were centrifuged and washed three times to remove any impurities or unreacted materials.

### 3.2. UV-Vis analysis of silver nanoparticles.

This study investigated the synthesis of Hs-AgNPs under various conditions, and UV-Vis analysis was performed (Figure 1).

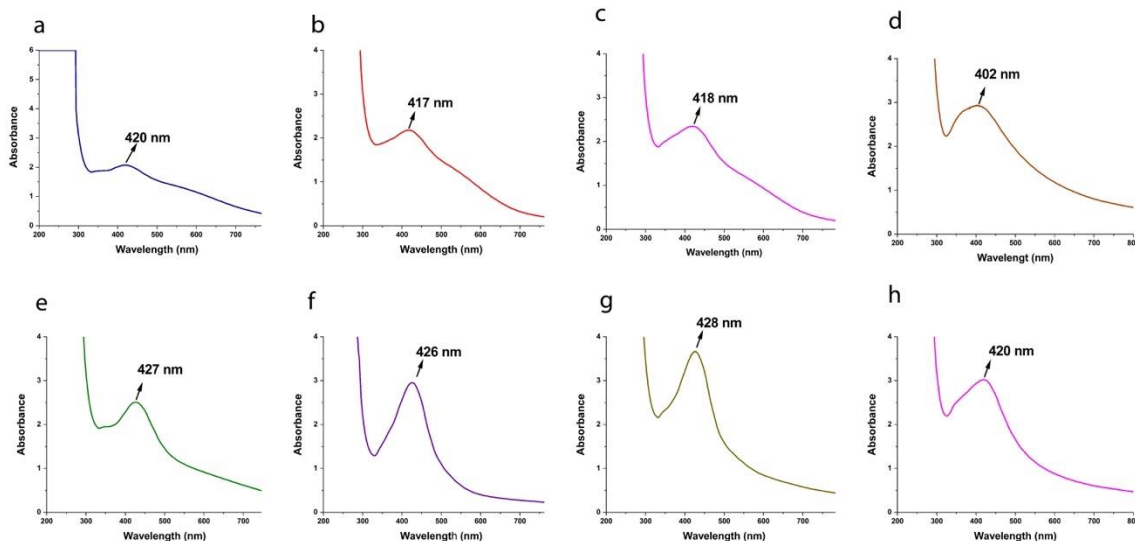


**Figure 1.** UV-Vis absorbance spectra of (a) Hs-AgNPs-1; (b) Hs-AgNPs-2; (c) Hs-AgNPs-3; (d) Hs-AgNPs-4; (e) Hs-AgNPs-5; (f) Hs-AgNPs-6; (g) Hs-AgNPs-7; (h) Hs-AgNPs-8.

UV-Vis spectrum analysis revealed distinct peak values and corresponding wavelengths for each sample. Hs-AgNPs-1 exhibited the highest peak value at a wavelength of 420 nm after 24 h, while Hs-AgNPs-2 and Hs-AgNPs-3 showed the highest peak values at wavelengths of 417 nm and 418 nm, respectively, after 320 min. Hs-AgNPs-4 displayed the highest peak value at a wavelength of 402 nm after 180 min. Furthermore, the impact of temperature on synthesis was explored, with Hs-AgNPs-5 synthesized at 50°C displaying the highest peak value at 427 nm after 150 minutes, indicating a decrease in synthesis time with increasing temperature. Hs-AgNPs-6, Hs-AgNPs-7, and Hs-AgNPs-8 exhibited the highest

peak values at wavelengths of 426 nm, 428 nm, and 420 nm, respectively, after 120 min. During the synthesis process, the UV-Vis spectrum changes were monitored at 15-minute intervals, and the synthesis was terminated when the peak value reached a certain level.

### 3.3. Characterization of silver nanoparticles by FTIR, XRD, and EDX analysis.

The FTIR analysis was conducted to determine the functional groups present in silver nanoparticles (Hs-AgNPs), as depicted in Figure 2a. The spectrum revealed several significant peaks that provide insights into the composition of the nanoparticles. The strong and broad peak observed at  $3369\text{ cm}^{-1}$  corresponds to the combined vibration frequency of the -OH and -NH<sub>2</sub> groups [37]. This indicates the presence of hydroxyl and amino groups, which are likely involved in the synthesis of AgNPs. The peak at  $2112\text{ cm}^{-1}$  can be attributed to the C-H bond [38], suggesting the presence of organic compounds in the nanoparticle structure. Another prominent peak observed at  $1643\text{ cm}^{-1}$  is indicative of C=C stretching. The peak at  $1537\text{ cm}^{-1}$  also represents the amide II bands, which arise from the combination of C-N stretching and N-H bending. These two peak values were found to be consistent across all nanoparticles, indicating the presence of specific functional groups in the Hs-AgNPs. Minor variations were observed in other bands, suggesting the presence of additional functional groups or slight structural differences among the nanoparticles. For instance, the band at  $1039\text{ cm}^{-1}$  represents the presence of alcohols, ethers, and carboxylic acids, indicating the involvement of these compounds in the synthesis process [39]. Based on these findings, it can be inferred that the formation of Ag nanoparticles is likely dependent on the reduction of hydroxyl groups present in phytochemicals. Furthermore, the stabilization of AgNPs may be facilitated by the presence of amino acids and proteins in the plant extract [40]. These functional groups and compounds contribute to the synthesis and stability of Hs-AgNPs.

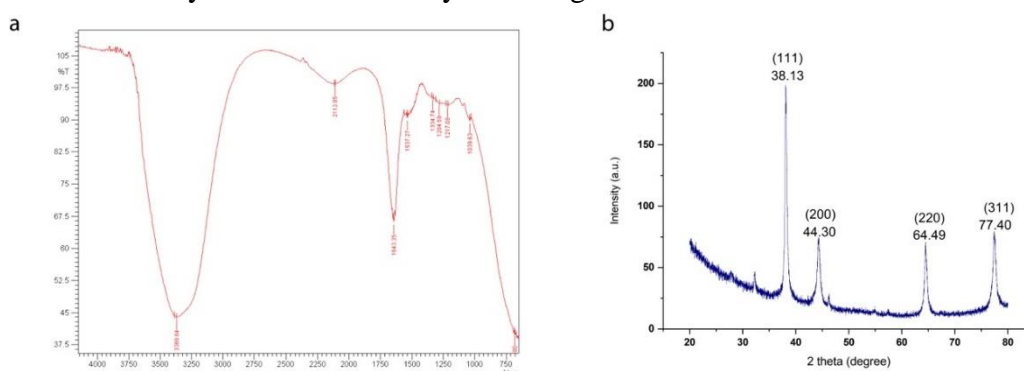


**Figure 2.** (a) Graphical representation from Infrared spectrum analysis; (b) XRD pattern of synthesized silver nanoparticles.

X-ray diffraction (XRD) technique was employed to determine the crystalline structure and elemental composition of Hs-AgNPs (Figure 2b). The XRD spectrum of the prepared AgNPs exhibited four diffraction bands at  $2\theta = 38.13, 44.30, 64.49,$  and  $77.40$ , corresponding to characteristic Bragg diffraction planes (111), (200), (220), and (310), respectively. These diffraction peaks revealed the crystalline nature of silver nanoparticles. These specific diffraction planes indicate the presence of well-defined crystallographic orientations in the AgNPs.

The FESEM was used to analyze nanoparticle sizes and shapes (Figure 3).

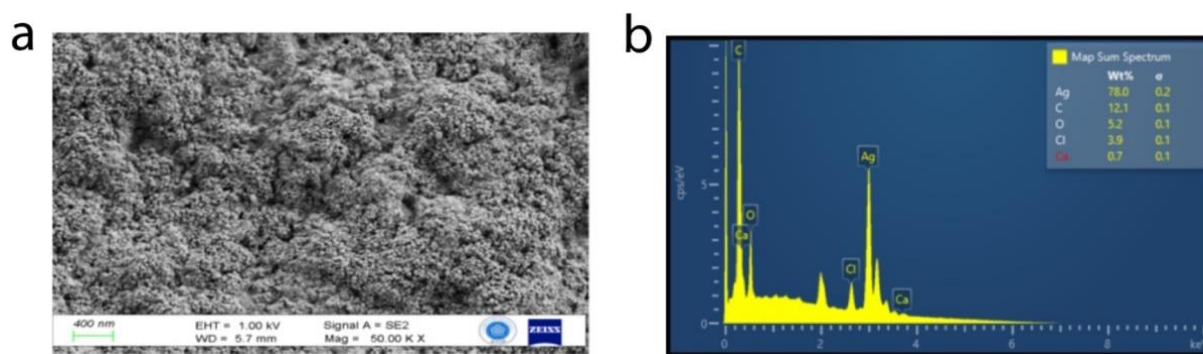


**Figure 3.** (a) FESEM image; (b) Energy-dispersive X-ray spectrometric pattern of synthesized silver nanoparticles.

The FESEM-EDX analysis shown in Figure 3b indicated the presence of a significant silver content. The EDX image of the synthesized AgNPs exhibited strong signals of the silver element. Additionally, the peak point of silver metal in the EDX measurement was detected in the range of  $\sim 3\text{--}4$  Kev, which is typically attributed to the optical absorption of silver nanoparticles due to their SPR (surface plasmon resonance) [41,42]. The EDX analysis revealed that the silver content accounted for approximately 78% of the composition. This high silver content confirms the successful synthesis of AgNPs and their purity.

#### 3.4. Analysis of size and zeta potentials of silver nanoparticles.

The synthesis of Hs-AgNPs was investigated under various conditions, and the results were analyzed regarding nanoparticle size and polydispersity index (PDI). Hs-AgNPs-1 exhibited an average nanoparticle size of 60.28 nm with a PDI value of 0.364 (Figure 4a). Changing the pH in Hs-AgNPs-2 to 8.5 decreased nanoparticle size to 34.31 nm but with a higher PDI value of 0.537 (Figure 4b). Increasing the  $\text{AgNO}_3$  concentration in Hs-AgNPs-3 to 2 mM further reduced the nanoparticle size to 29.95 nm, with a PDI value of 0.534 (Figure 4c). Hs-AgNPs-4, synthesized at a pH of 10.5, showed a slight decrease in average nanoparticle size to 28.71 nm (Figure 4d). The results indicated that the nanoparticle size decreased under room temperature synthesis conditions as the pH increased. In Hs-AgNPs-5, the only parameter that was changed from Hs-AgNPs-1 was the synthesis temperature, which was set at 50 °C. It was observed that the average nanoparticle size was 56.90 nm (Figure 4e). This result indicated that the temperature change, even with a slight decrease, reduced the nanoparticle size under pH 7.5. The PDI value for these nanoparticles was determined to be 0.296. This result indicated that the PDI values for Hs-AgNPs-1 and Hs-AgNPs-5 at pH 7.5 were lower, suggesting a more homogeneous size distribution of the nanoparticles. Nanoparticles with PDI values lower than 0.3 are expected to be more stable and exhibit a more homogeneous morphology, closely related to zeta potential [43]. Hs-AgNPs-6, synthesized at pH 8.5 and 50°C with a decreased plant extract concentration, exhibited an average nanoparticle size of 30.57 nm and a PDI value of 0.520 (Figure 4f). Increasing the plant extract concentration in Hs-AgNPs-7 resulted in a slight increase in nanoparticle size (32.38 nm) and a PDI value of 0.504 (Figure 4g). Finally, in Hs-AgNPs-8, synthesis at pH 10.5 and 50°C yielded a smaller nanoparticle size of 22.48 nm but with a higher PDI value of 0.571 (Figure 4h). These results indicate that pH,  $\text{AgNO}_3$  concentration, temperature, and plant extract concentration play significant roles in determining the size and homogeneity of the synthesized Hs-AgNPs.

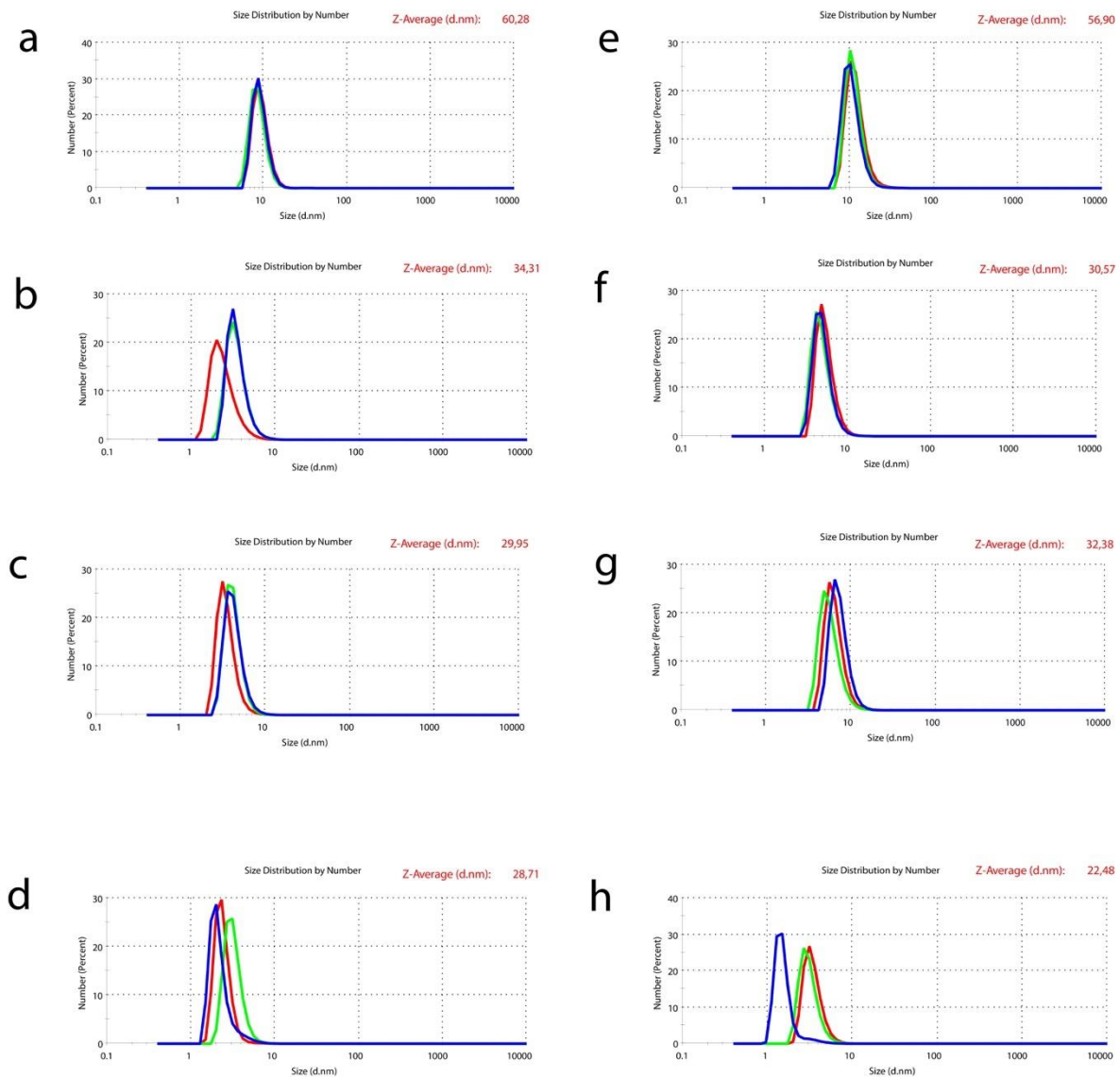


**Figure 4.** Size distribution of (a) Hs-AgNPs-1; (b) Hs-AgNPs-2; (c) Hs-AgNPs-3; (d) Hs-AgNPs-4; (e) Hs-AgNPs-5; (f) Hs-AgNPs-6; (g) Hs-AgNPs-7; (h) Hs-AgNPs-8.

DLS studies are primarily used to determine the particle size distribution and obtain the average hydrodynamic diameter of the samples [44]. The DLS size distribution analysis demonstrated that the pH, temperature, and AgNO<sub>3</sub> concentration significantly impacted the average size distribution of AgNPs during the synthesis process using *H. sabdariffa* extract, consistent with previous studies [43,45]. In the study conducted by Nouri *et al.* (2020), silver nanoparticles were synthesized using *Mentha aquatica* leaf extract to obtain ultra-small Ag nanoparticles [46]. Their study investigated the synthesis parameters such as pH, AgNO<sub>3</sub> concentration, and volume ratio of AgNO<sub>3</sub> solution to *Mentha aquatica* leaf extract for their effects on nanoparticle synthesis. Their results showed that a pH value of 9.5 yielded the best results in terms of nanoparticle synthesis. They found that the optimal volume ratio of AgNO<sub>3</sub> solution to *Mentha aquatica* leaf extract was 1:1. They also observed that increasing the reaction temperature led to a decrease in nanoparticle size and a faster reaction rate by indicating that the sample synthesized at room temperature (25°C) exhibited a high degree of nanoparticle monodispersity [46].

The zeta potentials of the synthesized nanoparticles were analyzed in Figure 5.

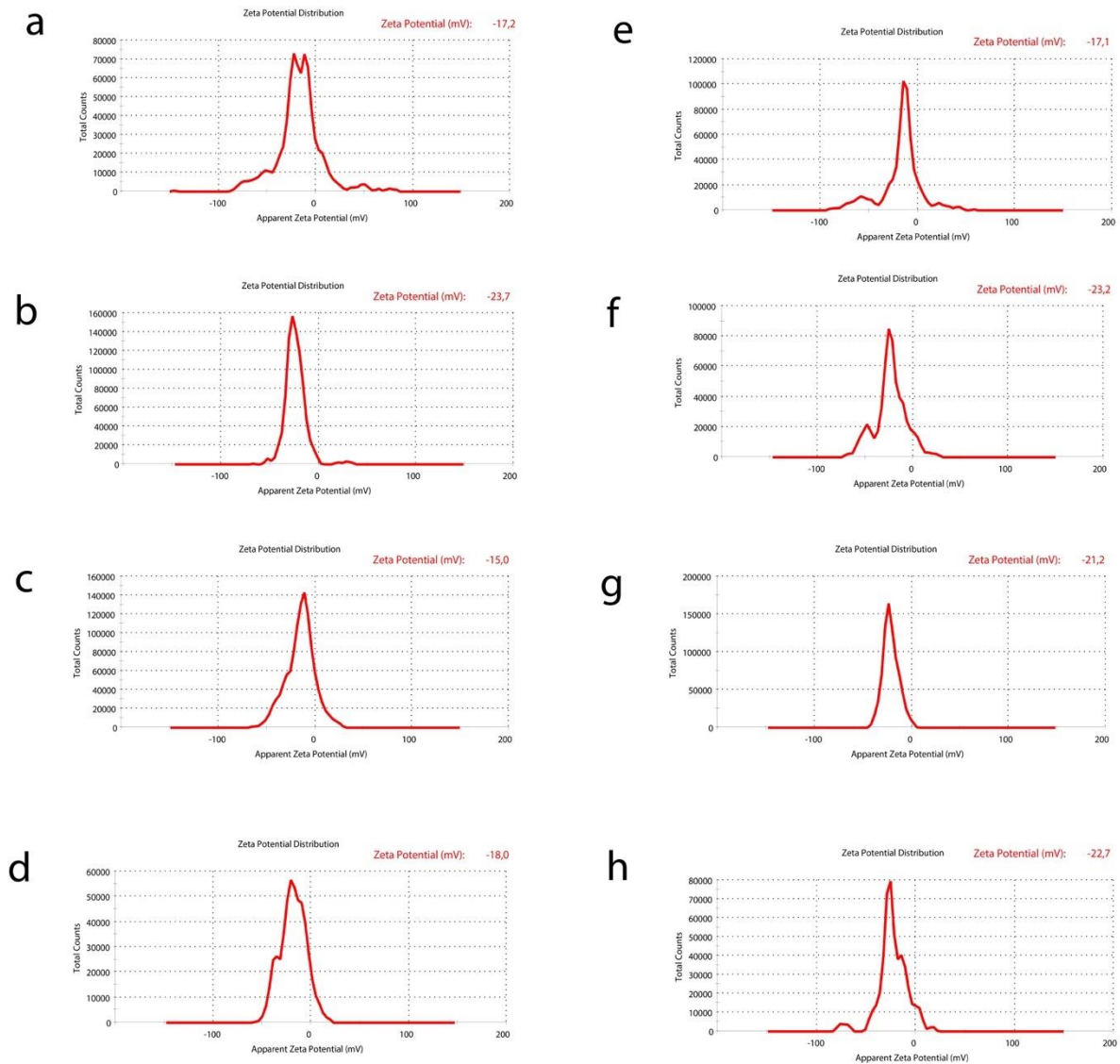


**Figure 5.** Zeta potential analysis of (a) Hs-AgNPs-1; (b) Hs-AgNPs-2; (c) Hs-AgNPs-3; (d) Hs-AgNPs-4; (e) Hs-AgNPs-5; (f) Hs-AgNPs-6; (g) Hs-AgNPs-7; (h) Hs-AgNPs-8.

For Hs-AgNPs-1, the zeta potential was determined to be -17.2. With an increase in pH, the zeta potential value for Hs-AgNPs-2 increased to -23.7, indicating the influence of pH on the zeta potential. For Hs-AgNPs-3, at pH 8.5, an increase in AgNO<sub>3</sub> concentration resulted in a zeta potential value of -15.0, highlighting the significant impact of AgNO<sub>3</sub> concentration on the zeta potential. Hs-AgNPs-4, with a pH of 10.5, exhibited a further decrease in zeta potential to -18.0 compared to Hs-AgNPs-3. When examining the zeta potential values at 50°C, Hs-AgNPs-5 showed a zeta potential of -17.1, like Hs-AgNPs-1, suggesting that temperature had a minimal effect on the zeta potential under pH 7.5. For Hs-AgNPs-6, the zeta potential was -23.2, while for Hs-AgNPs-7, it was -21.2, indicating that changes in pH decreased the zeta potential compared to Hs-AgNPs-5.

Additionally, a slight increase in zeta potential was observed for Hs-AgNPs-7 compared to Hs-AgNPs-6, attributed to the change in plant extract concentration. For Hs-AgNPs-8, at pH 10.5, the zeta potential was -22.7, showing a decrease compared to Hs-AgNPs-4. These results confirm the influence of pH on the zeta potential, as previously reported [47–49].

3.5. Shape analysis of silver nanoparticles by STEM.

In addition to the size analysis, the samples were also analyzed using a scanning transmission electron microscope (STEM) (Figure 6 and Figure 7).

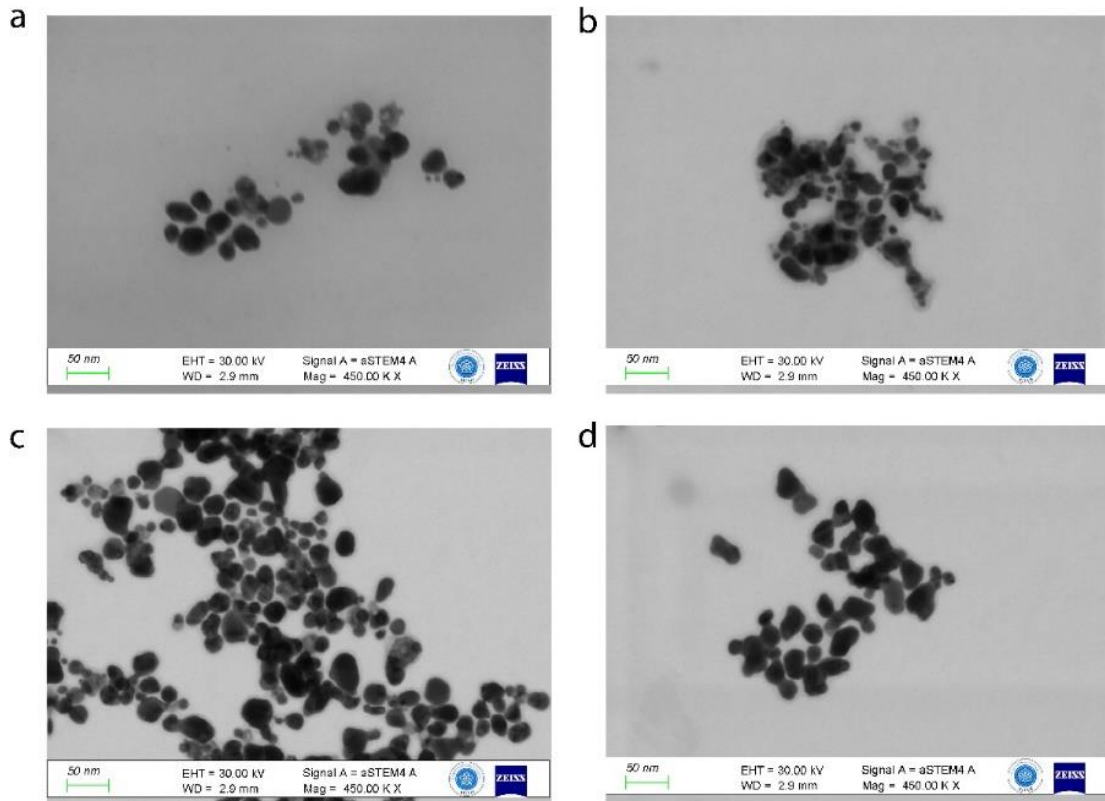


**Figure 6.** STEM images of (a) Hs-AgNPs-1; (b) Hs-AgNPs-2; (c) Hs-AgNPs-3; (d) Hs-AgNPs-4 synthesized at 25°C.

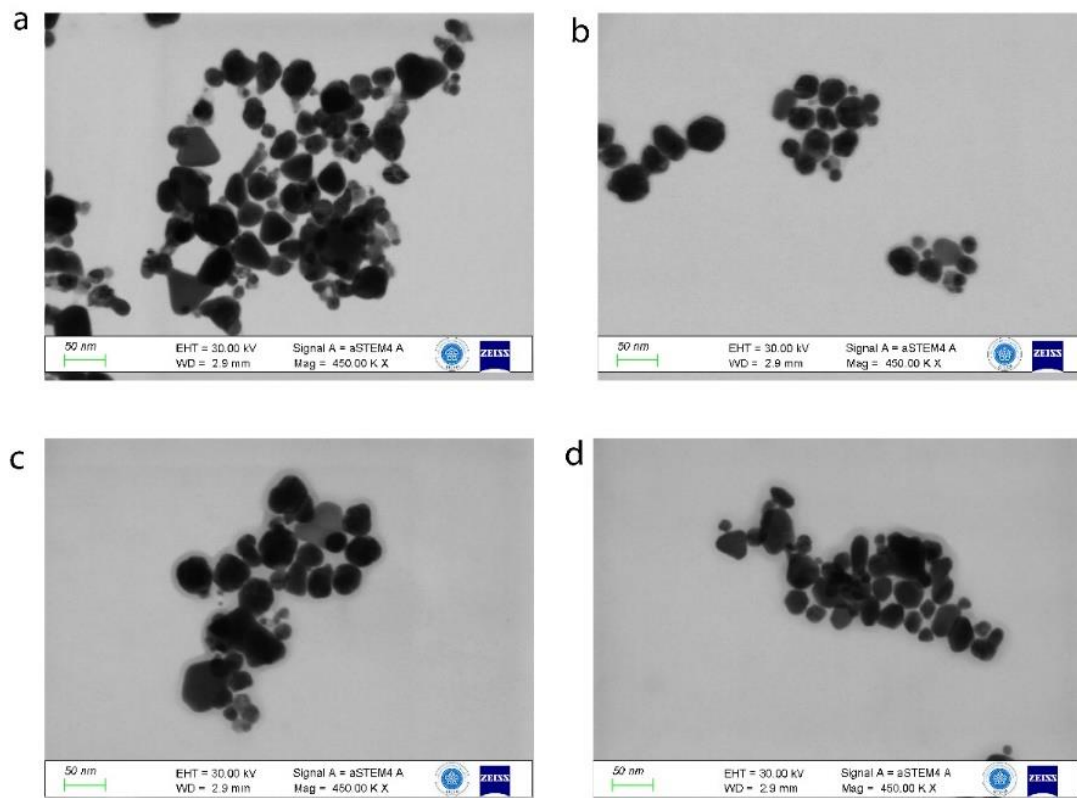


**Figure 7.** STEM images of (a) Hs-AgNPs-5; (b) Hs-AgNPs-6; (c) Hs-AgNPs-7; (d) Hs-AgNPs-8 synthesized at 50°C.

The shape analysis revealed that Hs-AgNPs-1, synthesized at pH 7.5, exhibited a more homogeneously distributed morphology, with the nanoparticles mostly appearing spherical. However, Hs-AgNPs-5 showed diversity in terms of shape. The STEM analysis provided visual confirmation of the size and shape of the synthesized silver nanoparticles. The observed spherical shape suggests the stability and uniformity of the nanoparticles. The variation in inhomogeneity and shape with changes in pH and synthesis conditions emphasizes the importance of controlling these parameters to achieve the desired characteristics of the nanoparticles. The STEM analysis supports the size and shape analysis findings, providing valuable insights into the morphology of the silver nanoparticles synthesized in this study.

3.6. Antimicrobial activity of synthesized silver nanoparticles.

The antimicrobial activity of silver nanoparticles (AgNPs) synthesized at 200 µg/mL concentration was evaluated using agar diffusion. The results showed that the synthesized AgNPs exhibited significant antibacterial and antifungal effects against various microorganisms (Table 2).

**Table 2.** Inhibition zones (diameter) in mm of the silver nanoparticles against tested bacterial strains by agar diffusion method.

Samples	Microorganisms							
	<i>S. aureus</i>	<i>B. cereus</i>	<i>E. coli</i>	<i>S. typhimurium</i>	<i>P. aeruginosa</i>	<i>B. subtilis</i>	<i>E. faecalis</i>	<i>A. niger</i>
Hs-AgNPs-1	18.77±0.59	12.91±0.58	11.58±0.43	13.73±1.17	12.36±0.62	14.03±0.43	15.14±0.24	16.67±0.72
Hs-AgNPs-2	18.72±0.53	12.47±0.73	11.90±0.62	13.91±0.56	12.89±0.82	14.09±0.29	13.77±0.71	13.02±0.35
Hs-AgNPs-3	18.96±0.60	13.52±0.13	12.67±0.65	13.97±0.74	12.56±0.35	14.44±0.56	14.17±0.43	12.38±1.25
Hs-AgNPs-4	–	–	–	–	–	–	–	–
Hs-AgNPs-5	18.29±0.86	13.05±1.13	10.74±0.41	13.93±0.64	12.49±0.34	13.54±0.59	15.04±0.70	13.42±0.40
Hs-AgNPs-6	8.95±0.48	–	10.44±0.11	11.71±0.70	–	–	10.72±0.94	–
Hs-AgNPs-7	9.69±0.18	9.73±0.71	11.69±0.92	12.88±0.25	10.06±0.42	–	10.88±0.46	–
Hs-AgNPs-8	–	–	–	–	–	–	–	–

The – Denotes no antibacterial activity. Individual data points were expressed in the form of mean ± standard deviation (mean ± SD).

Hs-AgNPs-3 consistently demonstrated the highest activity against *Staphylococcus aureus*, *Bacillus cereus*, *Escherichia coli*, *Salmonella typhimurium*, *Bacillus subtilis*, and *Enterococcus faecalis*, with inhibition zone values ranging from 8.95 ± 0.48 to 18.95 ± 0.59. In contrast, Hs-AgNPs-4 and 8 did not show any activity at this concentration. The observed variation in antimicrobial activity among different samples can be attributed to several factors, including pH, temperature, and extract concentration. Nanoparticles synthesized at room temperature and pH 7.5 and 8.5 generally exhibited better activity compared to those synthesized at pH 10.5. Among the nanoparticles synthesized at high temperatures, Hs-AgNPs-3 at pH 7.5 showed the highest activity. This suggests that the synthesis conditions, particularly the pH, play a crucial role in determining the antimicrobial efficacy of the nanoparticles. In the case of *Bacillus cereus*, Hs-AgNPs-1, 2, 3, and 5 showed similar antibacterial activity, while an increase in extract concentration resulted in antibacterial activity in Hs-AgNPs-7. However, Hs-AgNPs-6 did not show any activity against *Bacillus cereus*. Hs-AgNPs-4, 6, and 8 exhibited no activity against the respective microorganisms. Similar trends were observed in the antibacterial activity against *Escherichia coli*, *Salmonella typhimurium*, *Pseudomonas*

*aeruginosa*, and *Bacillus subtilis*. Hs-AgNPs-3 consistently showed the highest activity, while Hs-AgNPs-4 and 8 did not exhibit any activity against these microorganisms. In the case of *Enterococcus faecalis*, Hs-AgNPs-1 and 5 synthesized at pH 7.5 showed the highest inhibition zones, while Hs-AgNPs-4 and 8 did not show any activity. Regarding antifungal activity against *Aspergillus niger*, Hs-AgNPs-1 exhibited the highest activity with an inhibition zone value of  $16.14 \pm 0.72$  mm. Nanoparticles synthesized at pH 7.5 showed the highest antifungal activity, while Hs-AgNPs-4, 6, 7, and 8 did not exhibit any antifungal activity.

Previous studies have successfully demonstrated the synthesis of silver nanoparticles using the plant extract. One study utilized the leaf extract of *Hibiscus cannabinus* for the synthesis of silver nanoparticles. The effects of different concentrations of *H. cannabinus* leaf extract, metal ion concentrations, and reaction times on the synthesis of nanoparticles were evaluated. Additionally, they showed that the silver nanoparticles exhibited antimicrobial activity against *Escherichia coli*, *Proteus mirabilis*, and *Shigella flexneri* [50]. In another study, silver nanoparticles were synthesized at room temperature using the leaf extract of *Hibiscus sabdariffa*. The nanoparticles exhibited a distribution of various shapes and sizes ranging from approximately 5 nm to 60 nm [51]. In the study conducted by Manosalva *et al.* (2019), silver nanoparticles were successfully synthesized using *Galega officinalis* extract and AgNO<sub>3</sub> [43]. The optimization of the synthesis process of AgNPs showed that pH and AgNO<sub>3</sub> concentration significantly impacted the average size distribution of the nanoparticles. The variation of reaction parameters during the biosynthesis process led to forming AgNPs with different activities against *Escherichia coli*, *Staphylococcus aureus*, and *Pseudomonas syringae*. Particularly, they showed that AgNPs with a low size distribution demonstrated high efficacy against pathogenic microorganisms [43].

The findings of this study were consistent with previous research, which suggests that the initial pH of the medium, surface area, and shape of the nanoparticles play important roles in their antimicrobial activity. The results highlight the potential of silver nanoparticles as effective antimicrobial agents. All in all, the synthesized silver nanoparticles demonstrated significant antimicrobial activity against various microorganisms. The findings suggest that the synthesis conditions, particularly the pH, play a crucial role in determining the antimicrobial efficacy of the nanoparticles [52]

### 3.7. DPPH radical scavenging activities of synthesized silver nanoparticles.

The DPPH radical scavenging activities of the synthesized AgNPs at a concentration of 400 µg/mL were shown as percentage (%) values in Figure 8.

Ascorbic acid was used as a control. Sample 1 exhibited the highest antioxidant activity with a radical scavenging activity of  $70.05 \pm 2.88\%$ . It was found that AgNPs synthesized at pH 7.5 showed higher activity compared to nanoparticles synthesized under other conditions. The DPPH radical scavenging assay is commonly used to evaluate the antioxidant activity of nanoparticles[53,54]. The results of this study demonstrated that the synthesized AgNPs possess significant antioxidant activity. Sample 1 exhibited the highest radical scavenging activity, indicating its potential as an effective antioxidant.

The observed higher activity of AgNPs synthesized at pH 7.5 suggests that the synthesis conditions, particularly the pH, play a crucial role in determining the antioxidant efficacy of the nanoparticles. These findings were consistent with previous research, which has reported the antioxidant activity of silver nanoparticles synthesized under different conditions.

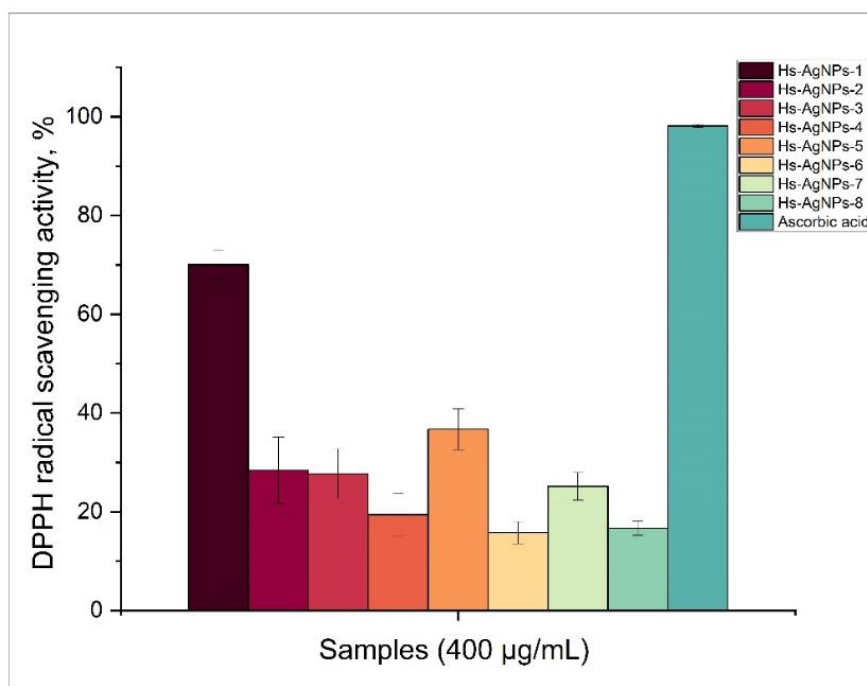


**Figure 8.** DPPH radical scavenging activity of silver nanoparticles synthesized using *Hibiscus sabdariffa* extract.

In the study conducted by J. Singh and Dhaliwal (2019), silver nanoparticles were synthesized using the toxic root extract of *Nepeta leucophylla* [55]. The effects of various synthesis parameters, such as root extract concentration, incubation time, temperature, and reaction pH, on the synthesis of silver nanoparticles were investigated in their study. They determined the optimized synthesis parameters with the optimum concentration of *N. leucophylla* root extract, which was found to be 20 mg/mL. They found that the silver nanoparticles synthesized at this concentration, using 1 mM silver nitrate at pH 9 and 50°C for 50 minutes, exhibited maximum antioxidant activity with a DPPH radical scavenging activity of  $79.41 \pm 0.004$  at a concentration of 250 µg/mL [55]. This study suggests that the synthesis conditions, particularly the pH, influence the antioxidant efficacy of the nanoparticles.

#### 4. Conclusions

The results showed that the wavelength of the nanoparticles decreased as the pH increased, as observed in the UV-Vis analysis. FTIR analysis indicated the role of phytochemicals in forming the nanoparticles and their potential involvement in stabilizing AgNPs. DLS analysis revealed the presence of highly homogeneous silver nanostructures at pH 7.5. The particle size of the nanoparticles decreased as the pH increased under room temperature synthesis conditions. Similarly, the nanoparticles' zeta potential was influenced by pH, AgNO<sub>3</sub> concentration, and extract concentration. The results of the zeta potential measurements provided insights into the surface charge, distribution, and stability of the AgNPs. Temperature was identified as another important factor in the synthesis of silver nanoparticles, as it controls the reaction kinetics of the synthetic process. The impact of temperature was examined by running the nanoparticle synthesis reaction at 50°C and room temperature. Among the synthesis parameters, the pH was found to have the most significant effect on the characteristic properties of the nanoparticles. The antimicrobial study further revealed that the synthesized nanoparticles (Hs-AgNPs) were effective against Gram-positive and Gram-negative bacteria. The highest activity was observed against *Staphylococcus aureus*,

suggesting potential applications in pharmacology and medicine. Generally, samples synthesized at lower pH values exhibited good antibacterial activity, while no antimicrobial activity was observed at pH 10.5.

Additionally, the extract concentration was found to influence the antibacterial efficacy. Overall, the results indicate that the reaction parameters significantly impact all the evaluated properties. From these findings, it can be concluded that the synthesis parameters of AgNPs play a crucial role in determining their characteristics, including size distribution, agglomeration, morphology, and biological activities.

## Funding

This research was funded by the Scientific Research Projects Coordination Unit of Necmettin Erbakan University, grant number 191315003.

## Acknowledgments

This study was conducted as part of Hasan BASARI's Master of Sciences thesis. The authors would like to extend their appreciation to Necmettin Erbakan University Science and Technology Research and Application Center (BITAM) for providing the necessary research infrastructure.

## Conflicts of Interest

The authors declare no conflict of interest. The funders had no role in the study's design, in the collection, analyses, or interpretation of data, in the writing of the manuscript, or in the decision to publish the results.

## References

1. Mukhopadhyay, R.; Kazi, J.; Debnath, M.C. Synthesis and characterization of copper nanoparticles stabilized with *Quisqualis indica* extract: Evaluation of its cytotoxicity and apoptosis in B16F10 melanoma cells. *Biomed. Pharmacother.* **2018**, *97*, 1373–1385, <https://doi.org/10.1016/j.biopha.2017.10.167>.
2. Paiva-Santos, A.C.; Herdade, A.M.; Guerra, C.; Peixoto, D.; Pereira-Silva, M.; Zeinali, M.; Mascarenhas-Melo, F.; Paranhos, A.; Veiga, F. Plant-mediated green synthesis of metal-based nanoparticles for dermatopharmaceutical and cosmetic applications. *Int. J. Pharm.* **2021**, *597*, 120311, <https://doi.org/10.1016/j.ijpharm.2021.120311>.
3. Wang, Q.; Chen, N.; Li, M.; Yao, S.; Sun, X.; Feng, X.; Chen, Y. Light-related activities of metal-based nanoparticles and their implications on dermatological treatment. *Drug Deliv. Transl. Res.* **2023**, *13*, 386–399, <https://doi.org/10.1007/s13346-022-01216-4>.
4. Vijayaram, S.; Razafindralambo, H.; Sun, Y.-Z.; Vasantharaj, S.; Ghafarifarsani, H.; Hoseinifar, S.H.; Raezadeh, M. Applications of green synthesized metal nanoparticles — a Review. *Biol. Trace Elem. Res.* **2024**, *202*, 360–386, <https://doi.org/10.1007/s12011-023-03645-9>.
5. Skrzyniarz, K.; Sanchez-Nieves, J.; de la Mata, F.J.; Łysek-Gładysińska, M.; Lach, K.; Ciepluch, K. Mechanistic insight of lysozyme transport through the outer bacteria membrane with dendronized silver nanoparticles for peptidoglycan degradation. *Int. J. Biol. Macromol.* **2023**, *237*, 124239, <https://doi.org/10.1016/j.ijbiomac.2023.124239>.
6. Li, W.-R.; Xie, X.-B.; Shi, Q.-S.; Zeng, H.-Y.; Ou-Yang, Y.-S.; Chen, Y.-B. Antibacterial activity and mechanism of silver nanoparticles on *Escherichia coli*. *Appl. Microbiol. Biotechnol.* **2010**, *85*, 1115–1122, <https://doi.org/10.1007/s00253-009-2159-5>.
7. Jeeva, K.; Thiyagarajan, M.; Elangovan, V.; Geetha, N.; Venkatachalam, P. *Caesalpinia coriaria* leaf extracts mediated biosynthesis of metallic silver nanoparticles and their antibacterial activity against

- clinically isolated pathogens. *Ind. Crops Prod.* **2014**, *52*, 714-720, <https://doi.org/10.1016/J.INDCROP.2013.11.037>.
8. Jinu, U.; Gomathi, M.; Saiqa, I.; Geetha, N.; Benelli, G.; Venkatachalam, P. Green engineered biomolecule-capped silver and copper nanohybrids using *prosopis cineraria* leaf extract: enhanced antibacterial activity against microbial pathogens of public health relevance and cytotoxicity on human breast cancer cells (MCF-7). *Microb. Pathog.* **2017**, *105*, 86–95, <https://doi.org/10.1016/J.MICPATH.2017.02.019>.
  9. Mousavi, S.M.; Hashemi, S.A.; Ghasemi, Y.; Atapour, A.; Amani, A.M.; Savar Dashtaki, A.; Babapoor, A.; Arjmand, O. Green synthesis of silver nanoparticles toward bio and medical applications: review study. *Artif. Cells Nanomed. Biotechnol.* **2018**, *46*, 855-872, <https://doi.org/10.1080/21691401.2018.1517769>.
  10. Sharma, V.K.; Yngard, R.A.; Lin, Y. Silver nanoparticles: Green synthesis and their antimicrobial activities. *Adv. Colloid Interface Sci.* **2009**, *145*, 83–96, <https://doi.org/10.1016/J.CIS.2008.09.002>.
  11. Xiu, Z.-m.; Zhang, Q.-b.; Puppala, H.L.; Colvin, V.L.; Alvarez, P.J.J. Negligible particle-specific antibacterial activity of silver nanoparticles. *Nano Lett.* **2012**, *12*, 4271-4275, <https://doi.org/10.1021/nl301934w>.
  12. Adeyemi, J.O.; Oriola, A.O.; Onwudiwe, D.C.; Oyedeji, A.O. Plant extracts mediated metal-based nanoparticles: synthesis and biological applications. *Biomolecules* **2022**, *12*, 627, <https://doi.org/10.3390/biom12050627>.
  13. Aswathi, V.P.; Meera, S.; Maria, C.G.A.; Nidhin, M. Green synthesis of nanoparticles from biodegradable waste extracts and their applications: a critical review. *Nanotechnol. Environ. Eng.* **2023**, *8*, 377–397, <https://doi.org/10.1007/s41204-022-00276-8>.
  14. Kutuk, Y.; Yontem, M.; Erci, F.; Esirgenler, B.; Isildak, I.; Totu, E.E. Plant extract mediated silver nanoparticles by concentrated sunlight and their antibacterial and cytotoxic activities. *Inorg. Nano-Met. Chem.* **2022**, 1–9, <https://doi.org/10.1080/24701556.2022.2074455>.
  15. Sharma, K.; Guleria, S.; Salaria, K.H.; Majeed, A.; Sharma, N.; Pawar, K.D.; Thakur, V.K.; Gupta, V.K. Photocatalytic and biological properties of silver nanoparticles synthesized using *Callistemon lanceolatus* leaf extract. *Ind. Crops Prod.* **2023**, *202*, 116951, <https://doi.org/10.1016/j.indcrop.2023.116951>.
  16. Luangpipat, T.; Beattie, I.R.; Chisti, Y.; Haverkamp, R.G. Gold nanoparticles produced in a microalga. *J. Nanoparticle Res.* **2011**, *13*, 6439–6445, <https://doi.org/10.1007/s11051-011-0397-9>.
  17. Saeed, S.; Iqbal, A.; Ashraf, M.A. Bacterial-mediated synthesis of silver nanoparticles and their significant effect against pathogens. *Environ. Sci. Pollut. Res.* **2020**, *27*, 37347–37356, <https://doi.org/10.1007/s11356-020-07610-0>.
  18. Erci, F.; Torlak, E. Antimicrobial and antibiofilm activity of green synthesized silver nanoparticles by using aqueous leaf extract of *Thymus serpyllum*. *Sakarya Univ. J. sci.* **2019**, *23*, 333–339, <https://doi.org/10.16984/saufenbilder.445146>.
  19. Abdel-Raouf, N.; Alharbi, R.M.; Al-Enazi, N.M.; Alkhulaifi, M.M.; Ibraheem, I.B.M. Rapid Biosynthesis of Silver Nanoparticles Using the Marine Red Alga *Laurencia Catarinensis* and Their Characterization. *Beni Suef Univ J Basic Appl Sci* **2018**, *7*, 150–157, <https://doi.org/10.1016/j.bjbas.2017.10.003>.
  20. Abdel-Raouf, N.; Alharbi, R.M.; Al-Enazi, N.M.; Alkhulaifi, M.M.; Ibraheem, I.B.M. Rapid biosynthesis of silver nanoparticles using the marine red alga *Laurencia catarinensis* and their characterization. *Beni-Suef Univ. J. Basic Appl. Sci.* **2018**, *7*, 150-157, <https://doi.org/10.1007/s42452-020-04046-6>.
  21. Mittal, A.K., Chisti, Y.; Banerjee, U.C. Synthesis of metallic nanoparticles using plant extracts. *Biotechnol. Adv.* **2013**, *31*, 346-356, <https://doi.org/10.1016/j.biotechadv.2013.01.003>.
  22. Pandit, C.; Roy, A.; Ghotekar, S.; Khusro, A.; Islam, M.N.; Emran, T.B.; Lam, S.E.; Khandaker, M.U.; Bradley, D.A. Biological agents for synthesis of nanoparticles and their applications. *J. King Saud Univ. Sci.* **2022**, *34*, 101869, <https://doi.org/10.1016/j.jksus.2022.101869>.
  23. Mittal, S.; Roy, A. 11 - Fungus and plant-mediated synthesis of metallic nanoparticles and their application in degradation of dyes. In *Photocatalytic Degradation of Dyes*, Shah, M., Dave, S., Das, J., Eds.; Elsevier: 2021; pp. 287-308, <https://doi.org/10.1016/B978-0-12-823876-9.00009-3>.
  24. Jeevanandam, J.; Kiew, S.F.; Boakye-Ansah, S.; Lau, S.Y.; Barhoum, A.; Danquah, M.K.; Rodrigues, J. Green approaches for the synthesis of metal and metal oxide nanoparticles using microbial and plant extracts. *Nanoscale* **2022**, *14*, 2534-2571, <https://doi.org/10.1039/D1NR08144F>.

25. Rani, N.; Singh, P.; Kumar, S.; Kumar, P.; Bhankar, V.; Kumar, K. Plant-mediated synthesis of nanoparticles and their applications: A review. *Mater. Res. Bull.* **2023**, *163*, 112233, <https://doi.org/10.1016/j.materresbull.2023.112233>.
26. Rolim, W.R.; Pelegrino, M.T.; de Araújo Lima, B.; Ferraz, L.S.; Costa, F.N.; Bernardes, J.S.; Rodrigues, T.; Brocchi, M.; Seabra, A.B. Green tea extract mediated biogenic synthesis of silver nanoparticles: Characterization, cytotoxicity evaluation and antibacterial activity. *Appl. Surf. Sci.* **2019**, *463*, 66-74, <https://doi.org/10.1016/j.apsusc.2018.08.203>.
27. Jiménez Pérez, Z.E.; Mathiyalagan, R.; Markus, J.; Kim, Y.-J.; Kang, H.M.; Abbai, R.; Seo, K.H.; Wang, D.; Soshnikova, V.; Yang, D.C. Ginseng-berry-mediated gold and silver nanoparticle synthesis and evaluation of their in vitro antioxidant, antimicrobial, and cytotoxicity effects on human dermal fibroblast and murine melanoma skin cell lines. *Int. J. Nanomed.* **2017**, *12*, 709-723, <https://doi.org/10.2147/IJN.S118373>.
28. Mahajan, M.; Kuiry, R.; Pal, P.K. Understanding the consequence of environmental stress for accumulation of secondary metabolites in medicinal and aromatic plants. *J. Appl. Res. Med. Aromat. Plants* **2020**, *18*, 100255, <https://doi.org/10.1016/j.jarmap.2020.100255>.
29. Erci, F.; Cakir-Koc, R.; Isildak, I. Green synthesis of silver nanoparticles using *Thymbra spicata* l. var. *spicata* (zahter) aqueous leaf extract and evaluation of their morphology-dependent antibacterial and cytotoxic activity. *Artif. Cells Nanomed. Biotechnol.* **2018**, *46*, 150-158, <https://doi.org/10.1080/21691401.2017.1415917>.
30. Hernández-Morales, L.; Espinoza-Gómez, H.; Flores-López, L.Z.; Sotelo-Barrera, E.L.; Núñez-Rivera, A.; Cadena-Nava, R.D.; Alonso-Núñez, G.; Espinoza, K.A. Study of the green synthesis of silver nanoparticles using a natural extract of dark or white *Salvia hispanica* L. seeds and their antibacterial application. *Appl. Surf. Sci.* **2019**, *489*, 952-961, <https://doi.org/10.1016/j.apsusc.2019.06.031>.
31. Arumai Selvan, D.; Mahendiran, D.; Senthil Kumar, R.; Kalilur Rahiman, A. Garlic, green tea and turmeric extracts-mediated green synthesis of silver nanoparticles: Phytochemical, antioxidant and *in vitro* cytotoxicity studies. *J. Photochem. Photobiol. B: Biol.* **2018**, *180*, 243-252, <https://doi.org/10.1016/j.jphotobiol.2018.02.014>.
32. Foudaa, A.; Saad, E.L.; Elgamala, M.S.; Mohamedb, A.A.; Salema, S.S. Optimal factors for biosynthesis of silver nanoparticles by *Aspergillus* sp. *Al Azhar Bull. Sci.* **2017**, *9*, 161-172.
33. Salem, S.S.; Fouda, A. Green synthesis of metallic nanoparticles and their prospective biotechnological applications: an overview. *Biol. Trace Elem. Res.* **2021**, *199*, 344-370, <https://doi.org/10.1007/s12011-020-02138-3>.
34. Benedec, D.; Oniga, I.; Cuibus, F.; Sevastre, B.; Stiufiuc, G.; Duma, M.; Hanganu, D.; Iacovita, C.; Stiufiuc, R.; Lucaciu, C.M. *Origanum vulgare* mediated green synthesis of biocompatible gold nanoparticles simultaneously possessing plasmonic, antioxidant and antimicrobial properties. *Int. J. Nanomed.* **2018**, *13*, 1041-1058, <https://doi.org/10.2147/IJN.S149819>.
35. Dada, A.O.; Adekola, F.A.; Dada, F.E.; Adelani-Akande, A.T.; Bello, M.O.; Okonkwo, C.R.; Inyinbor, A.A.; Oluyori, A.P.; Olayanju, A.; Ajanaku, K.O. Silver nanoparticle synthesis by *Acalypha wilkesiana* extract: phytochemical screening, characterization, influence of operational parameters, and preliminary antibacterial testing. *Heliyon* **2019**, *5*, e02517, <https://doi.org/10.1016/j.heliyon.2019.e02517>.
36. Gubitosa, J.; Rizzi, V.; Lopodota, A.; Fini, P.; Laurenzana, A.; Fibbi, G.; Fanelli, F.; Petrella, A.; Laquintana, V.; Denora, N.; Comparelli, R.; Cosma, P. One pot environmental friendly synthesis of gold nanoparticles using *Punica Granatum* Juice: A novel antioxidant agent for future dermatological and cosmetic applications. *J. Colloid Interface Sci.* **2018**, *521*, 50-61, <https://doi.org/10.1016/j.jcis.2018.02.069>.
37. Noruzi, M.; Zare, D.; Khoshnevisan, K.; Davoodi, D. Rapid green synthesis of gold nanoparticles using *Rosa hybrida* petal extract at room temperature. *Spectrochim. Acta - A: Mol. Biomol. Spectrosc.* **2011**, *79*, 1461-1465, <https://doi.org/10.1016/J.SAA.2011.05.001>.
38. Tsegay, M.G.; Gebretinsae, H.G.; Sackey, J.; Maaza, M.; Nuru, Z.Y. Green synthesis of khat mediated silver nanoparticles for efficient detection of mercury ions. *Mater. Today Proc.* **2021**, *36*, 368-373, <https://doi.org/10.1016/J.MATPR.2020.04.217>.
39. Khan, M.R.; Hoque, S.M.; Hossain, K.F.B.; Siddique, M.A.B.; Uddin, M.K.; Rahman, M.M. Green synthesis of silver nanoparticles using *Hibiscus sabdariffa* leaf extract and its cytotoxicity assay. *Inorg. Nano-Met. Chem.* **2022**, 1-11, <https://doi.org/10.1080/24701556.2021.2025091>.

40. Da-Costa-Rocha, I.; Bonnlaender, B.; Sievers, H.; Pischel, I.; Heinrich, M. *Hibiscus aabdariffa* L. – A phytochemical and pharmacological review. *Food Chem.* **2014**, *165*, 424–443, <https://doi.org/10.1016/J.FOODCHEM.2014.05.002>.
41. Kalimuthu, K.; Suresh Babu, R.; Venkataraman, D.; Bilal, M.; Gurunathan, S. Biosynthesis of silver nanocrystals by *Bacillus licheniformis*. *Colloids Surf. B: Biointerfaces* **2008**, *65*, 150-153, <https://doi.org/10.1016/J.COLSURFB.2008.02.018>.
42. Chakraborty, B.; Bhat, M.P.; Basavarajappa, D.S.; Rudrappa, M.; Nayaka, S.; Kumar, R.S.; Almansour, A.I.; Perumal, K. Biosynthesis and characterization of polysaccharide-capped silver nanoparticles from *Acalypha indica* L. and evaluation of their biological activities. *Environ. Res.* **2023**, *225*, 115614, <https://doi.org/10.1016/j.envres.2023.115614>.
43. Manosalva, N.; Tortella, G.; Cristina Diez, M.; Schalchli, H.; Seabra, A.B.; Durán, N.; Rubilar, O. Green synthesis of silver nanoparticles: effect of synthesis reaction parameters on antimicrobial activity. *World J. Microbiol. Biotechnol.* **2019**, *35*, 88, <https://doi.org/10.1007/s11274-019-2664-3>.
44. Rajeshkumar, S.; Bharath, L.V. Mechanism of plant-mediated synthesis of silver nanoparticles – A review on biomolecules involved, characterisation and antibacterial activity. *Chem. Biol. Interact.* **2017**, *273*, 219–227, <https://doi.org/10.1016/J.CBI.2017.06.019>.
45. Velgosová, O.; Mražíková, A.; Marcinčáková, R. Influence of pH on green synthesis of Ag nanoparticles. *Mater. Lett.* **2016**, *180*, 336-339, <https://doi.org/10.1016/J.MATLET.2016.04.045>.
46. Nouri, A.; Tavakkoli Yarak, M.; Lajevardi, A.; Rezaei, Z.; Ghorbanpour, M.; Tanzifi, M. Ultrasonic-assisted green synthesis of silver nanoparticles using *Mentha aquatica* leaf extract for enhanced antibacterial properties and catalytic activity. *Colloid Interface Sci. Commun.* **2020**, *35*, 100252, <https://doi.org/10.1016/j.colcom.2020.100252>.
47. Jiang, W.; Mashayekhi, H.; Xing, B. Bacterial toxicity comparison between nano- and micro-scaled oxide particles. *Environ. Pollut.* **2009**, *157*, 1619–1625, <https://doi.org/10.1016/J.ENVPOL.2008.12.025>.
48. Khan, S.S.; Mukherjee, A.; Chandrasekaran, N. Impact of exopolysaccharides on the stability of silver nanoparticles in water. *Water Res.* **2011**, *45*, 5184–5190, <https://doi.org/10.1016/J.WATRES.2011.07.024>.
49. Peng, Z.G.; Hidajat, K.; Uddin, M.S. Adsorption of bovine serum albumin on nanosized magnetic particles. *J. Colloid Interface Sci.* **2004**, *271*, 277–283, <https://doi.org/10.1016/J.JCIS.2003.12.022>.
50. Bindhu, M.R.; Umadevi, M. Synthesis of monodispersed silver nanoparticles using *Hibiscus cannabinus* leaf extract and its antimicrobial activity. *Spectrochim. Acta A Mol. Biomol. Spectrosc.* **2013**, *101*, 184–190, <https://doi.org/10.1016/J.SAA.2012.09.031>.
51. Kalita, N.K.; Ganguli, J.N. *Hibiscus sabdariffa* L. leaf extract mediated green synthesis of silver nanoparticles and its use in catalytic reduction of 4-nitrophenol. *Inorg. Nano-Met. Chem.* **2017**, *47*, 788–793, <https://doi.org/10.1080/15533174.2016.1218506>.
52. Nayak, R.R.; Pradhan, N.; Behera, D.; Pradhan, K.M.; Mishra, S.; Sukla, L.B.; Mishra, B.K. Green synthesis of silver nanoparticle by *Penicillium purpurogenum* NPMF: the process and optimization. *J. Nanoparticle Res.* **2011**, *13*, 3129-3137, <https://doi.org/10.1007/s11051-010-0208-8>.
53. Erenler, R.; Gecer, E.N.; Hosaflioglu, I.; Behcet, L. Green synthesis of silver nanoparticles using *Stachys spectabilis*: identification, catalytic degradation, and antioxidant activity. *Biochem. Biophys. Res. Commun.* **2023**, *659*, 91–95, <https://doi.org/10.1016/j.bbrc.2023.04.015>.
54. Gulcin, İ.; Alwasel, S.H. DPPH Radical Scavenging Assay. *Processes* **2023**, *11*, 2248, <https://doi.org/10.3390/pr11082248>.
55. Singh, J.; Dhaliwal, A.S. Novel green synthesis and characterization of the antioxidant activity of silver nanoparticles prepared from *Nepeta leucophylla* Root Extract. *Anal. Lett.* **2019**, *52*, 213–230, <https://doi.org/10.1080/00032719.2018.1454936>.